Proceedings of the 2025 SICE Festival with Annual Conference
September 9-12, 2025, Chiang Mai, Thailand

Dynamical Network Biomarker Analysis of Biomolecular PID Control Systems Exhibiting Saddle-Node Bifurcation

Ryouhei Nishiguchi,[1] Takashi Nakakuki,[1] and Jun-ichi Imura[2]

Abstract— **Diabetes progression is increasingly hypothesized to involve the breakdown of homeostasis—a biological feedback regulation—which may be associated with a bifurcation phenomenon. The dynamical network biomarker (DNB) theory aims to detect qualitative state transitions associated with bifurcation phenomena by identifying DNB nodes whose fluctuations increase near critical points. However, identifying DNB nodes is challenging under high-dimensional and low-sample-size conditions. In this study, we focused on a biomolecular PID feedback control system—referred to as aPID—that exhibits saddle-node bifurcation, assuming that it underlies homeostatic regulation. We analytically show that the aPID controller state inherently satisfies DNB conditions at the bifurcation onset, enabling the a priori identification of DNB nodes without the need for exhaustive data-driven analysis.**

I. Introduction

The global prevalence of chronic diseases—including diabetes, cardiovascular diseases, and cancer—has steadily increased in recent decades. According to the latest IDF Diabetes Atlas (2025), approximately 590 million individuals are living with diabetes, a figure that is projected to exceed 853 million by 2050 [1]. This alarming trend underscores the urgent need for innovative strategies to better understand, monitor, and manage the mechanisms underlying diabetes progression. Recent studies have revealed that the progression of diabetes is associated with the dysfunction of biological regulatory mechanisms, collectively known as homeostasis, across complex interorgan networks [2], [3]. Building on these findings, attention has increasingly turned to the breakdown of homeostasis in metabolic systems, formulated within the framework of complex systems theory, which has been linked to qualitative changes in internal biological feedback mechanisms, such as the antithetic integral feedback (AIF) mechanism [4].

In particular, the dynamical network biomarker (DNB) theory has attracted growing attention [6]. This theory interprets the breakdown of feedback control as a bifurcation phenomenon arising from variations in specific parameters within biological systems [5]. Because bifurcation point prediction in the DNB theory is based on observing fluctuations in the time-series responses of a set of state variables, referred to as DNB nodes, the problem of predicting bifurcation points is essentially reduced to the identification of DNB nodes within a dynamical system.

However, biological systems are fundamentally high-dimensional and nonlinear, making it technically challenging to comprehensively observe all the states of such complex systems at sufficiently high temporal resolutions to identify DNB nodes. Alternatively, DNB nodes can be identified from the elements of the eigenvector corresponding to the eigenvalue closest to the imaginary axis in the Jacobian matrix, which is derived by linearizing the system to its operating point [8]. However, because it is nearly impossible to obtain an accurate mathematical model of a high-dimensional and nonlinear biological system, it is extremely difficult to estimate the corresponding Jacobian matrix, particularly in situations where only high-dimensional, low-sample-size (HDLSS) data are available [7]. This limitation presents a major obstacle to the practical application of DNB-based early warning methods in real biological systems.

In this study, we addressed the challenge of identifying DNB nodes not through data-driven methods—which are often constrained by the high-dimensional, low-sample-size (HDLSS) nature of biological data—but through a model-based analytical approach. Assuming that homeostasis in metabolic systems is maintained via a biomolecular PID control mechanism (aPID) that can exhibit saddle-node bifurcation, we theoretically demonstrate that at least one of the controller's internal state variables always satisfies the defining conditions of a DNB node as the system approaches bifurcation. This insight enables the a priori identification of DNB nodes, solely based on the system's structure, eliminating the need for an exhaustive data-driven search across all variables. The effectiveness of the proposed framework was further validated through numerical simulations based on a glucose-insulin regulatory model incorporating an aPID mechanism.

II. Preliminaries

A. Dynamical network biomarker

In this section, we outline DNB analysis applied to systems that exhibit saddle-node bifurcations.

Consider the following nonlinear system:

$$\dot{\xi} = f(\xi, p) + w, \tag{1}$$

where $\xi \in \mathbb{R}^n$ and $p \in \mathbb{R}$ represent the state vector and the bifurcation parameter, respectively, $f : \mathbb{R}^n \times \mathbb{R} \to \mathbb{R}^n$ is a continuously differentiable and nonlinear function, and $w \in \mathbb{R}^n$ is Gaussian white noise with the covariance matrix $D \in \mathbb{R}^{n \times n}$.

Let ξ^* denote the equilibrium point of interest in the nonlinear system, and introduce the following linearized system in its neighborhood:

$$\dot{x} = Jx + w, \tag{2}$$

[1]Department of Intelligent and Control Systems, Kyushu Institute of Technology, Japan nakakuki@ics.kyutech.ac.jp

[2]Department of Systems and Control Engineering, School of Engineering, Institute of Science Tokyo, Japan imura.j.6486@m.isct.ac.jp

where $x = [x_1, x_2, ..., x_n]^\top = \xi - \xi^*$ and $J = (\partial f(\xi, p)/\partial \xi)|_{\xi=\xi^*} \in \mathbb{R}^{n\times n}$ is the Jacobian matrix evaluated at ξ^*. For DNB analysis in the case of saddle-node bifurcation, the following assumption was imposed:

Assumption 1: All eigenvalues of the Jacobian matrix J have negative real parts prior to bifurcation, and the eigenvalue closest to the imaginary axis is real. Furthermore, the matrix J is assumed to be diagonalizable.

Let $\lambda_d \in \mathbb{R}$ be the largest eigenvalue of the Jacobian matrix J, and let v_d be the corresponding eigenvector, referred to as the MAC eigenvector [7]. Thus, the following relationship holds [8]:

$$\lim_{\lambda_d \to 0-} (-2\lambda_d) C = \tilde{D}(v_d v_d^\top), \tag{3}$$

where $C \in \mathbb{R}^n$ is the covariance matrix of x at the equilibrium point of interest and $\tilde{D} \in \mathbb{R}$ is a finite positive constant. Equation (3) indicates that as λ_d tends to zero, the (i, j)-th element of the covariance matrix C diverges provided that the i-th and j-th elements of v_d are nonzero. Therefore, denoting the ith element of v_d by $v_d(i)$, as the bifurcation parameter p of system (1) approaches the critical point, the fluctuation of x_{i^*} increases markedly for all $i^* \in \{i \in \mathbb{N} | v_d(i) \neq 0\}$, where $\mathbb{N}$ denotes a set of natural numbers. These variables are referred to as DNBs.

B. Antithetic PID feedback control

Consider the biomolecular reaction system described by the following equation:

$$\dot{x} = S\lambda + ue_1, \tag{4}$$

where $x = [x_1, x_2, \ldots, x_n]^\top \in \mathbb{R}^n$ represents the state vector, x_i $(i = 1, 2, \ldots, n)$ denotes the concentration of chemical species X_i, $S \in \mathbb{Z}^{n\times r}$ is the stoichiometry matrix, and $\lambda : \mathbb{R}^n \to \mathbb{R}^r$ is a vector-valued propensity function described by reaction rate laws such as mass-action or Michaelis–Menten kinetics. Without loss of generality, we assume that the input stimulus u is applied to state x_1, where $e_1 = [1, 0, \ldots, 0]^\top$. In addition, the state variable regulated through feedback, that is, the system output, is denoted by x_n.

We now consider the design problem of a feedback controller for system (4) that regulates the state variable x_n to a target concentration. To this end, a PID controller implementable at the biomolecular level can be expressed, for example, by the following equation [9]:

$$\begin{cases} \dot{z}_1 = \mu + k_D x_n - \eta z_1 z_2, \\ \dot{z}_2 = \theta x_n - \eta z_1 z_2, \\ u = h_{\mathrm{pi}}(z_i, x_1, x_n; k_P, k_I), \end{cases} \tag{5}$$

where z_1 and z_2 are the state variables of the controller; μ, θ, and η are positive constants; k_P, k_I, and k_D are non-negative PID parameters; and $h_{\mathrm{pi}} : \mathbb{R} \times \mathbb{R} \times \mathbb{R} \to \mathbb{R}$ is a function designed to appropriately realize the PID mechanism (see [9] for details, and also Section 4 for an example). Here, for the function $h_{\mathrm{pi}}(z_i, \cdots)$, if the polarity of the input-output gain is positive (N-type system), then $i = 1$; if it is negative (P-type system), then $i = 2$.

Then, the feedback law (5), referred to as the antithetic PID (aPID) controller, is shown to achieve a robust perfect adaptation, provided that the closed-loop system is Lyapunov stable.

III. Results

A. Formulation of the aPID feedback control system

Consider a closed-loop system comprising an n-dimensional biomolecular reaction system (plant) and a 2nd order aPID controller:

$$\text{plant:} \begin{cases} \dot{x}_1 &= f_1(x, z; k_P, k_I), \\ &\vdots \\ \dot{x}_n &= f_n(x, z; k_P, k_I), \end{cases} \tag{6}$$

$$\text{controller:} \begin{cases} \dot{z}_1 &= \mu + h_{\mathrm{d}}(x_n; k_D) - \eta z_1 z_2, \\ \dot{z}_2 &= \theta x_n - \eta z_1 z_2, \end{cases} \tag{7}$$

where $x = [x_1, \cdots x_n]^\top \in \mathbb{R}^n$ and $z = [z_1, z_2]^\top \in \mathbb{R}^n$ are the state vectors of the plant and the aPID controller, respectively, and $f_i : \mathbb{R}^n \times \mathbb{R}^2 \to \mathbb{R}$ $(i = 1, \ldots, n)$ denotes the reaction rate function for the i-th species. Without loss of generality, the state variable regulated by the controller is assumed to be x_n. The controller parameters μ, θ, and η are positive constants; k_P, k_I, and k_D are non-negative PID parameters; and $h_d(x_n; k_D) = k_D x_n$ or $h_d(x_n; k_D) = k_D x_n^2$.

If the equilibrium point of the closed-loop system is Lyapunov stable, a robust perfect adaptation of x_n is achieved. Specifically, the steady-state value of x_n is given by

$$\lim_{t\to\infty} x_n = \frac{\mu}{\theta - k_D}, \quad (0 \leq k_D < \theta) \tag{8}$$

for the case $h_d(x_n; k_D) = k_D x_n$, and

$$\lim_{t\to\infty} x_n = \frac{\theta \pm \sqrt{\theta^2 - 4k_D\mu}}{2k_D}, \quad \left(0 \leq k_D < \frac{\theta^2}{4\mu}\right) \tag{9}$$

for the case $h_d(x_n; k_D) = k_D x_n^2$.

Remark 1: In Eq. (4), the control input u is applied only to the state variable x_1 because of the structure of e_1. By contrast, as shown in Eq. (6), this study considers a more general setting in which the input can act on all state variables. Moreover, the analysis was conducted in a unified manner without distinguishing between P- and N-type plants.

Remark 2: Regarding the equilibrium point, we have $z_1^* \neq 0$ and $z_2^* \neq 0$. Suppose $z_1^* = 0$. Then, from Eq. (7), we obtain

$$\dot{z}_1 = \mu + h_d(x_n; k_D) \geq \mu > 0,$$

which contradicts the equilibrium condition $\dot{z}_1 \equiv 0$. Therefore, $z_1^* \neq 0$ must hold. A similar argument applies to z_2^*.

B. DNB analysis of the aPID feedback control system

1) Properties of state variables in the aPID controller: For the aPID feedback control system (6)–(7), let the equilibrium point of interest be given by $(x,z) = (x^*, z^*)$. The Jacobian matrix obtained by linearizing the system at the equilibrium point is given by

$$J = \left[\begin{array}{ccc|cc} a_{11} & \cdots & a_{1n} & b_{11} & b_{12} \\ \vdots & \ddots & \vdots & \vdots & \vdots \\ a_{n1} & \cdots & a_{nn} & b_{n1} & b_{n2} \\ \hline 0 & \cdots & c_{1n} & -\eta z_2^* & -\eta z_1^* \\ 0 & \cdots & \theta & -\eta z_2^* & -\eta z_1^* \end{array}\right] = \left[\begin{array}{c|c} A & B \\ \hline C & D \end{array}\right], \tag{10}$$

where the elements are

$$a_{ij} = \left.\frac{\partial f_i}{\partial x_j}\right|_{(x*,z*)} \quad (i,j = 1,\cdots,n), \tag{11}$$

$$b_{ik} = \left.\frac{\partial f_i}{\partial z_k}\right|_{(x*,z*)} \quad (i = 1,\cdots,n; k = 1,2), \tag{12}$$

$$c_{1n} = \left.\frac{\partial h_d}{\partial x_n}\right|_{x_n^*}, \tag{13}$$

and the matrices are of dimensions $A \in \mathbb{R}^{n\times n}$, $B \in \mathbb{R}^{n\times 2}$, $C \in \mathbb{R}^{2\times n}$, and $D \in \mathbb{R}^{2\times 2}$.

In addition to Assumption 1, we make the following assumptions:

Assumption 2: The matrix A is non-singular, and the matrix B is nonzero.

Remark 3: While the non-singularity of the matrix A appears to be reasonable in the context of real biomolecular systems, it may still become singular when conservation laws are present in the reaction network. In such cases, the matrix A can be regularized by reducing the system's dimensionality using the conservation laws.

Remark 4: If the matrix B is zero, the aPID controller becomes completely decoupled from the plant, resulting in a degenerate case that should be excluded from the analysis.

In the saddle-node bifurcation considered under Assumption 1, the largest eigenvalue λ_d of the Jacobian matrix J asymptotically approaches zero as the system nears the bifurcation point. As both the Jacobian matrix and the corresponding MAC-eigenvector vary continuously with respect to the bifurcation parameter [10], DNBs can be identified by examining the eigenvector v_0 associated with the zero eigenvalue $\lambda_0 = 0$ of J. In this context, the following theorem holds for the state variables of the aPID controller.

Theorem 1: Consider the aPID feedback control system (6)–(7). Suppose that Assumptions 1 and 2 hold for the Jacobian matrix derived by linearizing the system at the equilibrium point of interest (x^*, z^*), as given in Eq. (10). Then, at least one of the aPID controller state variables, z_1 or z_2, qualifies as a DNB.

Proof: Suppose that a saddle-node bifurcation occurs, at which point the Jacobian matrix (10) has a zero eigenvalue $\lambda_0 = 0$:

$$Jv_0 = \lambda_0 v_0 = 0, \quad v_0 := \begin{bmatrix} v_{0_1} \\ v_{0_2} \\ v_{0_3} \end{bmatrix} = \begin{bmatrix} v_{0_{11}} \\ \vdots \\ v_{0_{1n}} \\ v_{0_2} \\ v_{0_3} \end{bmatrix} \in \mathbb{R}^{n+2}, \tag{14}$$

where $v_{0_1} = [v_{0_{11}}, v_{0_{12}}, \ldots, v_{0_{1n}}]^\top \in \mathbb{R}^n$ denotes the subvector of the eigenvector v_0 corresponding to the state variables of the plant, and v_{0_2} and $v_{0_3} \in \mathbb{R}$ denote the elements of v_0 corresponding to the state variables of the aPID controller.

If $v_{0_2} = v_{0_3} = 0$, then from Eqs. (10) and (14), it follows that $Av_{0_1} = 0$, which contradicts the non-singularity of the matrix A. Therefore, at least one of the elements v_{0_2} or v_{0_3} must be nonzero.

We now investigate in more detail the conditions that v_{0_2} and v_{0_3} must satisfy when the Jacobian matrix has a zero eigenvalue. By performing a row operation on the $(n+1)$st row of Eq. (14), we obtain the following relationship:

$$z_2^* v_{0_2} + z_1^* v_{0_3} = 0. \tag{15}$$

Conversely, as the matrix A is nonsingular by Assumption 2, the determinant of the Jacobian matrix $|J|$ can be transformed as follows, using the Schur complement formula:

$$|J| = |A||D - CA^{-1}B|, \quad |A| \neq O. \tag{16}$$

Then, we can see that

$$\begin{aligned} |D - CA^{-1}B| = \eta z_2^*(c_2A^{-1}b_2 - c_1A^{-1}b_2) \\ +\eta z_1^*(c_1A^{-1}b_1 - c_2A^{-1}b_1), \end{aligned} \tag{17}$$

where b_1 and b_2 denote the first and second columns of the matrix B, and c_1 and c_2 denote the first and second rows of the matrix C, respectively. It should be noted that the following identity, which is beneficial in simplifying the derivation, was used:

$$(c_1A^{-1}b_1)(c_2A^{-1}b_2) - (c_2A^{-1}b_1)(c_1A^{-1}b_2) = 0.$$

As the Jacobian matrix has a zero eigenvalue if and only if $|J| = 0$, from (17), we have

$$z_2^*(c_2A^{-1}b_2 - c_1A^{-1}b_2) = z_1^*(c_2A^{-1}b_1 - c_1A^{-1}b_1). \tag{18}$$

When $(c_2A^{-1}b_2 - c_1A^{-1}b_2) \neq 0$, Eqs. (15) and (18) yield:

$$z_1^*\left(\frac{c_2A^{-1}b_1 - c_1A^{-1}b_1}{c_2A^{-1}b_2 - c_1A^{-1}b_2}v_{02} + v_{0_3}\right) = 0. \tag{19}$$

As $z_1^* \neq 0$ (see Remark 2), we obtain the following relation:

$$\begin{bmatrix} v_{0_2} \\ v_{0_3} \end{bmatrix} = \alpha \begin{bmatrix} 1 \\ -\dfrac{c_2A^{-1}b_1 - c_1A^{-1}b_1}{c_2A^{-1}b_2 - c_1A^{-1}b_2} \end{bmatrix}, \tag{20}$$

where α is an arbitrary constant.

Similarly, if $(c_2A^{-1}b_1 - c_1A^{-1}b_1) \neq 0$, then we obtain the following equation:

$$\begin{bmatrix} v_{0_2} \\ v_{0_3} \end{bmatrix} = \alpha \begin{bmatrix} -\dfrac{c_2A^{-1}b_2 - c_1A^{-1}b_2}{c_2A^{-1}b_1 - c_1A^{-1}b_1} \\ 1 \end{bmatrix}. \tag{21}$$

From the discussion above, at least one of v_{0_2} or v_{0_3} must be nonzero. Let the MAC-eigenvector be defined as

$$v_d := \begin{bmatrix} v_{d_1} \\ v_{d_2} \\ v_{d_3} \end{bmatrix} = \begin{bmatrix} v_{d_{11}} \\ \vdots \\ v_{d_{1n}} \\ v_{d_2} \\ v_{d_3} \end{bmatrix} \in \mathbb{R}^{n+2}, \tag{22}$$

Then, by the continuity of eigenvectors near the saddle-node bifurcation, at least one of v_{d_2} or v_{d_3} is also nonzero, implying that at least one of the aPID controller state variables z_1 or z_2 becomes a DNB. ■

Remark 5: Theorem 1 is particularly important for practical applications of the DNB theory. For example, if energy metabolism homeostasis is maintained by an aPID feedback control mechanism, then the problem of identifying DNBs can be reduced to identifying the organs or regulatory modules in which the aPID controller is implemented. This significantly narrows the search space compared to the conventional approach of detecting DNBs from a vast number of state variables in complex interorgan control systems.

2) Properties of the state variables in the plant: As a direct consequence of Theorem 1, we obtain the following results for the state variables of the plant.

Corollary 1: The state variable, x_n, which is regulated by the controller, cannot serve as a DNB.

Proof: From the $(n+1)$st and $(n+2)$nd rows of equation $Jv_0 = 0$, we obtain

$$c_{1n} v_{0_{1n}} - \eta z_2^* v_{02} - \eta z_1^* v_{03} = 0, \tag{23}$$
$$\theta v_{0_{1n}} - \eta z_2^* v_{02} - \eta z_1^* v_{03} = 0. \tag{24}$$

Considering the difference between these two equations, we obtain the following equation:

$$(\theta - k_D) v_{0_{1n}} = 0, \tag{25}$$

for the case $h_d(x_n; k_D) = k_D x_n$. As the PID parameter is designed to satisfy $k_d < \theta$, it follows that $v_{0_{1n}} = 0$.

Similarly, for case $h_d(x_n; k_D) = k_D x_n^2$, we have

$$(\theta - 2k_D x_n^*) v_{0_{1n}} = (\pm\sqrt{\theta^2 - 4k_D\mu}) v_{0_{1n}} = 0. \tag{26}$$

As $k_D < \theta^2/(4\mu)$, it follows that $v_{0_{1n}} = 0$.

Owing to the continuity of eigenvectors, the n-th element of the MAC-eigenvector also satisfies $v_{d_{1n}} = 0$. Therefore, it can be concluded that the regulated output x_n cannot serve as a DNB because its fluctuation does not increase near the bifurcation point. ■

Remark 6: This conclusion is significant for the application of the DNB theory. For example, if homeostasis in energy metabolism is achieved through aPID feedback control mechanism, observing fluctuations in the regulated output, such as blood-borne factors (e.g., glucose), does not enable the prediction of the bifurcation point.

IV. Numerical Verification

A. Glucose-insulin regulatory model

To validate our theoretical results, we considered the glucose-insulin regulatory model originally proposed in [11], which we extended by incorporating an aPID feedback control mechanism. This modified model enabled us to examine the emergence of saddle-node bifurcations under the influence of a biologically plausible control structure.

$$\begin{cases} \dot{I} = \sigma\left(\dfrac{k_{I_2} z_2^2}{K_{I_2} + z_2^2}\right)\left(\dfrac{k_P G^2}{K_P + G^2}\right) - kI, \\ \dot{G} = R_0\left(\dfrac{k_{I_1} z_1^2}{K_{I_1} + z_1^2}\right) - (E_{G0} + S_I I)\, G, \\ \dot{z}_1 = \mu + k_D G^2 - \eta z_1 z_2, \\ \dot{z}_2 = \theta G - \eta z_1 z_2, \end{cases} \tag{27}$$

where I and G represent the concentrations of insulin and glucose, respectively, and constitute the state variables of the plant. The controller variables z_1 and z_2 are interpreted as abstract regulatory factors involved in the modulation of glucagon and insulin secretion within α cells and β cells, respectively. The system parameters obtained from Ref. [11] are summarized in Table I, except for E_{G0}, which was modified from the original value ($E_{G0} = 1.44$) to suit the bifurcation analysis. The control parameters used in this study are listed in Table II. In this simulation, the target value (reference) was set to a blood glucose concentration of $G \simeq 75$ [mg/dL].

B. Simulation of control failure caused by saddle-node bifurcation

In this setting, E_{G0} acts as a bifurcation parameter, with saddle-node bifurcation occurring near $E_{G0} \simeq 0.21$. At this point, the control system lost its ability to maintain the target glucose level, leading to a steady-state deviation. Figures 2 show the time responses of the system variables (G, I, z_1, and z_2) before and after the bifurcation, which are hypothesized to correspond to a healthy physiological state and a transition to a disease state, respectively. The red dashed line represents target blood glucose levels. We observed that before bifurcation, the aPID controller functioned

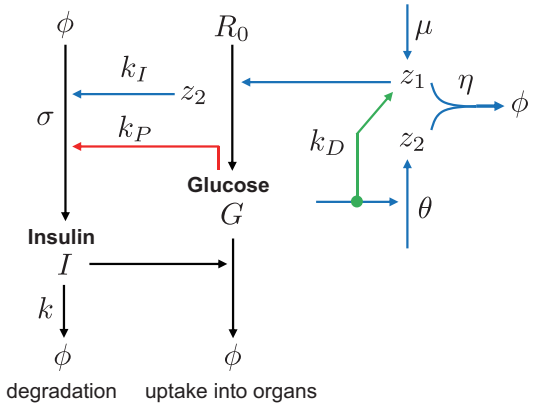

Fig. 1. Glucose-insulin regulatory model with aPID feedback mechanism

TABLE I

SYSTEM PARAMETERS

Parameters	Values	Units
S_I	0.72	$mL\ \mu\ U^{-1}d^{-1}$
E_{G0}	5	d^{-1}
R_0	864	$mgdL^{-1}d^{-1}$
σ	43.2	$\mu UmL^{-1}d^{-1}$
k	432	d^{-1}

TABLE II

CONTROLLER PARAMETERS

Parameters	Values
k_P	1
K_P	50
k_{I_1}	1
K_{I_1}	0.01
k_{I_2}	10
K_{I_2}	10000
k_D	0.1
μ	7000
θ	100
η	0.01

properly and successfully regulated the blood glucose level to the target value of $G \simeq 75$ [mg/dL], which corresponds to the analytically derived steady-state value of $G = 75.74$ [mg/dL] as given by Eq. (9). However, after the bifurcation, the controller failed to maintain regulation, resulting in a significant deviation from the target level.

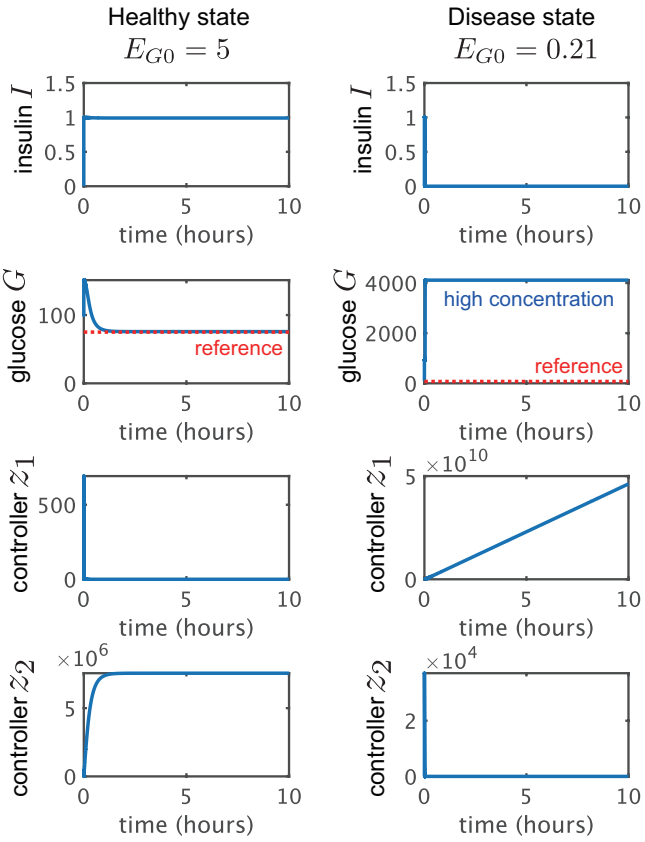

Fig. 2. Time responses before and after the bifurcation ($E_{G0} = 5$ vs. 0.21)

C. Verification of DNB characteristics in the aPID feedback control system

To validate the theoretical predictions presented in Theorem 1 and Corollary 1, we conducted a numerical analysis based on the DNB theory. Specifically, we evaluated the fluctuations in the state variables to examine whether they exhibit DNB characteristics near the bifurcation point.

First, we identified the parameter setting immediately before the onset of the bifurcation as $E_{G0} = 0.22$. We computed the corresponding equilibrium point as $(I^*, G^*, z_1^*, z_2^*) = (0.991, 75.7, 0.0299, 25300000)$, satisfying Assumption 1:

Then, the Jacobian matrix J evaluated at the corresponding equilibrium point is given by

$$J = \begin{bmatrix} -432 & 0.0977 & 0 & 0 \\ -54.5 & -0.934 & 4350 & 0 \\ 0 & 15.1 & -2.54 \times 10^5 & -2.99 \times 10^{-4} \\ 0 & 100 & -2.54 \times 10^5 & -2.99 \times 10^{-4} \end{bmatrix}. \tag{28}$$

For submatrix A of the Jacobian matrix J, we have $|A| \simeq 409 \neq 0$. In addition, the submatrix B is a nonzero matrix, thereby confirming that Assumption 2 is satisfied.

Finally, the eigenvalues of the Jacobian matrix are computed as $\lambda = \{-2.5 \times 10^5,\ -4.3 \times 10^2,\ -6.9 \times 10^{-1},\ -6.3 \times 10^{-4}\}$, indicating that $\lambda_d = -6.3 \times 10^{-4}$ has the largest eigenvalue. Then, the corresponding MAC-eigenvector v_d is given by

$$v_d = \begin{bmatrix} -1.7 \times 10^{-9} \\ -7.5 \times 10^{-6} \\ -1.6 \times 10^{-9} \\ 1 \end{bmatrix}. \tag{29}$$

This result shows that the fourth element of the MAC-eigenvector is not only nonzero, but also significantly larger than the others, indicating that the controller state variable z_2 exhibits the characteristics of a DNB node near the bifurcation point. In contrast, the second element of the MAC-eigenvector, which corresponds to the output variable G, is relatively small, as expected. Moreover, we confirmed that the second element rapidly decreased as the bifurcation parameter approached the critical value. Therefore, output variable G of the controlled plant does not exhibit DNB characteristics.

D. Observation of fluctuation responses

In the DNB theory, in addition to analyzing the MAC-eigenvector, DNB nodes can be estimated from the fluctuation responses of the system near its equilibrium point. Figure3 shows the fluctuation responses around the operating point of the aPID control system before the bifurcation ($E_{G0} = 5$) and just prior to the bifurcation ($E_{G0} = 0.22$), respectively. The simulations were performed using MATLAB/Simulink, where noise was introduced via a Band-Limited White Noise block that generated random numbers

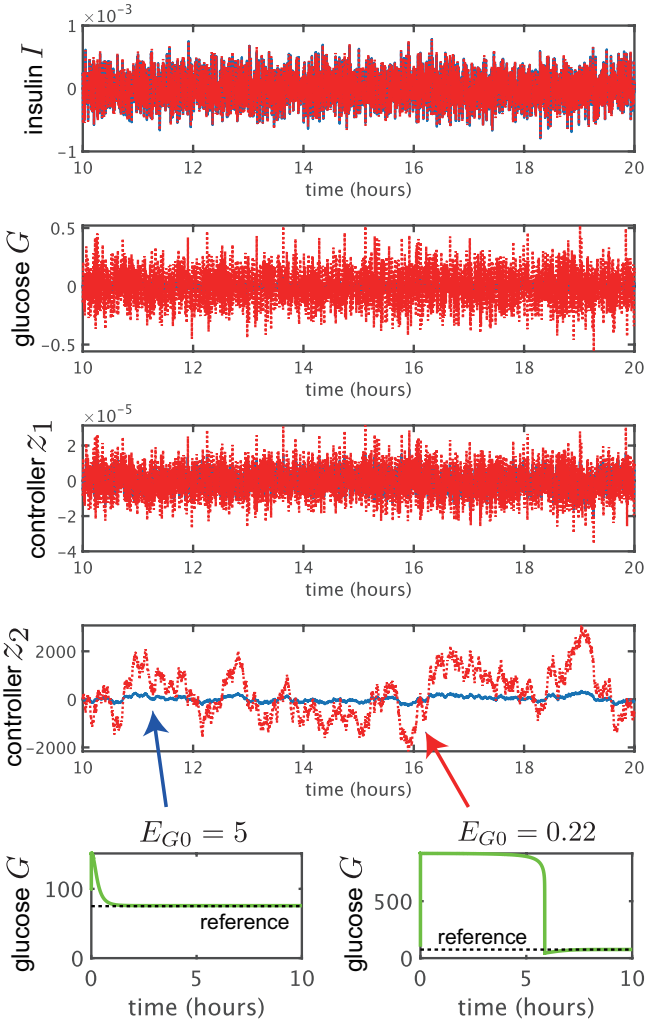

Fig. 3. Fluctuation responses of the system before ($E_{G0} = 5$) and just before ($E_{G0} = 0.22$) the bifurcation

based on a normal distribution.

The figure shows that the fluctuation response of z_2 increases as the system approaches the bifurcation point, exhibiting the characteristic behavior of a DNB. By contrast, the fluctuation response of G shows no significant change, indicating that it does not exhibit DNB characteristics. Similarly, the responses of I and z_1 also remain relatively unchanged, further supporting the absence of DNB behavior in these variables. These results agree well with the theoretical predictions of Theorem 1 and Corollary 1.

V. Conclusions

In this study, we examined the theoretical relationship between DNBs and aPID feedback control systems that exhibit saddle-node bifurcation. We analytically demonstrated that under general assumptions, at least one of the internal state variables of the aPID controller—either z_1 or z_2—inevitably becomes a DNB at the onset of bifurcation. Conversely, the controlled output variable x_n is proven to not become a DNB, regardless of the system's proximity to the bifurcation.

This result significantly improved the efficiency of DNB identification in complex biological systems, particularly under HDLSS conditions. In practice, this enables the reduction of the DNB search space from a vast array of system variables to a small, functionally interpretable subset, namely, the variables directly involved in regulatory control mechanisms, such as aPID.

We validated our theoretical findings using a modified glucose-insulin regulation model to include an aPID feedback loop. The simulation results confirmed that bifurcation leads to a loss of robust perfect adaptation in glucose concentration, with significant fluctuations observed in the controller state z_2 prior to bifurcation, while the output variable G remained stable. This supports the conclusion that controller states—not controlled outputs—serve as early warning indicators of system destabilization.

Overall, the results presented in this paper provide a promising model-based foundation for applying the DNB theory to real biological systems, offering a tractable and theoretically grounded method for detecting early warning signals of homeostatic breakdowns, such as those occurring during diabetes progression.

VI. Acknowledgements

This research was supported by JST Moonshot R&D (grant number JPMJMS2021).

References

[1] International Diabetes Federation, IDF Diabetes Atlas 11th Edition. Available from: https://diabetesatlas.org/resources/idf-diabetes-atlas-2025/

[2] H. Katagiri, Inter-organ communication involved in metabolic regulation at the whole-body level. Inflamm Regen, Vol. 43, No. 1:60, 2023.

[3] K. Takahashi, T. Yamada and H. Katagiri, Inter-Organ Communication Involved in Brown Adipose Tissue Thermogenesis. In: Tominaga, M., Takagi, M. (eds) Thermal Biology, *Advances in Experimental Medicine and Biology*, Vol. 1461, Springer, Singapore, 2024.

[4] M. H. Khammash, Perfect adaptation in biology, *Cell Syst*, Vol. 12, No. 6, pp. 509–521, 2021.

[5] K. Aihara, R. Liu, K. Koizumi, X. Liu and L. Chen, Dynamical network biomarkers: Theory and applications, *Gene*, Vol. 808, 145997, 2022.

[6] L. Chen, R. Liu, ZP. Liu, M. Li and K. Aihara, Detecting early-warning signals for sudden deterioration of complex diseases by dynamical network biomarkers, *Scientific Reports*, Vol. 2, No. 342, 2012.

[7] X. Shen, H. Sasahara, J. Imura, M. Oku and K. Aihara, Re-Stabilizing Large-Scale Network Systems Using High-Dimension Low-Sample-Size Data Analysis, *in IEEE Transactions on Emerging Topics in Computational Intelligence*, Vol. 9, No. 2, pp. 1638–1649, 2025.

[8] M. Oku and K. Aihara, On the covariance matrix of the stationary distribution of a noisy dynamical system, *Nonlinear Theory and Its Applications*, Vol. 9, No. 2, pp. 166–184, 2018.

[9] M. Filo, S. Kumar and M. Khammash, A hierarchy of biomolecular proportional-integral-derivative feedback controllers for robust perfect adaptation and dynamic performance, *Nature Communications*, Vol. 13, 2022.

[10] T-S. Han, M. Iri, Jordan normal form, The University of Tokyo Press, 1982 (in Japanese).

[11] B. Topp, K. Promislow, G. Devries, R. M. Miura and D. T. Finegood, A Model of β-Cell Mass, Insulin, and Glucose Kinetics: Pathways to Diabetes, *Journal of Theoretical Biology*, Vol. 206, No. 4, pp. 605-619, 2000.